RECENT ELECTROANALYTICAL STUDIES IN MOLTEN FLUORIDES

D. L. Manning* and Gleb Mamantov**

*Analytical Chemistry Division, Oak Ridge National Laboratory†
Oak Ridge, Tennessee 37830

**Department of Chemistry, The University of Tennessee
Knoxville, Tennessee 37916

1. INTRODUCTION

We have been interested for some time (1-32) in the application of modern electroanalytical methods to the study of molten fluoride salt systems of interest to nuclear reactor technology. The development of in situ (in-line) monitoring techniques has been one of the main goals of this research. An obvious advantage of in-line monitoring is that it would provide immediate knowledge of the behavior of the reactor fuel and at the same time eliminate sampling and other time consuming procedures. Experience with this and other programs has generally demonstrated the value of in-line analysis, both in more economical analyses and, frequently, in more timely and meaningful results.

Electroanalytical methods appear to be especially attractive for the direct analysis of electroactive species in molten salt reactor fuel and coolant salt systems. This chapter summarizes our electroanalytical studies of bismuth, iron tellurium, oxide and U(IV)/U(III) ratio determinations in molten LiF-BeF_2-ThF_4 (72-16-12 mole %) and LiF-BeF_2-ZrF_4 (65.6-29.4-5.0 mole %). These salts are the Molten Salt Breeder Reactor (MSBR) and Molten Salt Reactor (MSR) fuel solvents, respectively (33).

---

†Operated by the Union Carbide Corporation for the Energy Research and Development Administration.

2. EXPERIMENTAL

The experimental set-ups for voltammetric and chronopotentiometric studies in molten fluorides have been described previously (7,32). The controlled potential-controlled current cyclic voltammeter is described elsewhere (34). A Tektronix 7313 storage oscilloscope equipped with a series C-50/C-70 Polaroid Camera, and a Hewlett-Packard Model 7045-A X-Y recorder were used to record the voltammograms and chronopotentiograms. The melts were contained in glassy carbon crucibles (obtained from Beckwith Corp., Van Nuys, California). Gold, iridium, pyrolytic graphite and glassy carbon unsheathed working electrodes were used (typical area approx. 0.25 cm^2), as well as iridium quasi-reference electrodes (6). The Ni(II)/Ni reference electrode (11,20,23) was not employed in order to simulate in-line monitoring conditions involving highly radioactive melts under which the use of this electrode may prove impractical. The glassy carbon crucible was used as the counter electrode. The solvent salts, LiF-BeF_2-ThF_4 and LiF-BeF_2-ZrF_4, were prepared and purified by Chemical Technology Division personnel at the Oak Ridge National Laboratory. The procedures have been reported previously (35). Bismuth, nickel and iron were added as anhydrous BiF_3, NiF_2 and FeF_2, respectively. Oxide was added as either sublimed Al_2O_3 (36) or "low fired" BeO (37). The peroxide and superoxide were added as high purity Na_2O_2 and NaO_2, respectively.

Tellurium compounds, Li_2Te and $LiTe_3$, were prepared by members of the Chemistry Division, Oak Ridge National Laboratory (38).

3. RESULTS AND DISCUSSION

Bismuth

Bismuth, because of its potential use in MSBR fuel reprocessing (39), is a potential trace level impurity in a reactor fuel stream. Under such conditions bismuth will probably be present in the metallic state, so that some oxidative pretreatment would be necessary before carrying out a voltammetric determination of bismuth. The electroreduction of Bi(III) in molten LiF-BeF_2-ZrF_4 by voltammetry and chronopotentiometry was first studied by Hammond and Manning (26). This work pointed to the need for additional investigations on the behavior of bismuth mainly in the areas of instability of Bi(III) in the melts, the extent of interference from nickel and the feasibility of extending the limits of detection of bismuth below that of linear scan voltammetry.

As noted previously (26) stable solutions of Bi(III) in molten LiF-BeF_2-ZrF_4 could not be maintained for extended periods of time

(days) in either graphite or copper cells. The two main routes for the loss appeared to be reduction of Bi(III) by the container material and/or volatilization as BiF_3. For further investigations of bismuth in molten $LiF-BeF_2-ZrF_4$, a melt containing Bi(III) at a concentration of about 10 mM was set up where the melt was contained in a glassy carbon crucible. Well defined voltammograms and chronopotentiograms were obtained at gold, iridium and glassy carbon electrodes. The peak potential for Bi(III) reduction occurs at about -0.1 V vs Ir QRE (prior results (26) showed that this reduction occurs at approx. + 0.1 V vs Ni(II)/Ni reference electrode). Again, however, the bismuth was slowly lost from the melt as revealed by a gradual decrease in the voltammetric peak current with time. To check for volatilization, a cold finger was placed in the cell for a few days; an X-ray fluorescence analysis of the deposited film revealed that the major constituent was indeed bismuth. Thus, it now appears that bismuth is slowly lost from molten $LiF-BeF_2-ZrF_4$ primarily by volatilization; this result is in agreement with the work of Cubicciotti (40).

Because nickel is an anticipated interference, the effect of nickel on the bismuth voltammograms was determined while sufficient bismuth (approximately 5 mM) remained to produce well-defined curves. Nickel as NiF_2 was added to give a Ni(II) concentration of 15 mM. The reduction of Bi(III) precedes that of Ni(II) by $\sim$ 200mV under these conditions (see Figure 1, upper curve); this separation appeared to be sufficient for the determination of low concentrations of Bi(III) in the presence of typical concentrations of Ni(II) (41), particularly if derivative methods are employed.

The Ni(II) reduction wave (E_p = -.25V in Figure 1, upper curve) is poorly defined; however, two clearly separated stripping peaks were obtained on reverse scans. The first peak probably corresponds to the oxidation of Ni or possibly Ni-Bi alloy; the second peak at $\sim$ 0V corresponds to stripping of bismuth from the electrode. When the scan is started to an initial potential of about +0.4 V vs Ir QRE, a small prewave is seen, which, although not completely understood, is believed to result from the adsorption of bismuth at the electrode surface. The middle voltammogram of Figure 1 corresponds to about 10 ppm (0.11mM) Bi(III) and 240 ppm (15mM) Ni(II). The bismuth reduction wave has practically disappeared, and only one broad stripping peak (largely due to nickel) is present. The prewave, which is shown on an expanded scale in the lower curve of Figure 1, did not change significantly.

The slow loss of bismuth from the melt at 600°C was followed voltammetrically; the concentration of Bi(III) decreased from approximately 400 ppm (4.4mM) to about 7 ppm (0.077mM) in 40 days. This is about the lowest concentration that can be measured by direct linear-scan voltammetry in these melts. Anodic stripping

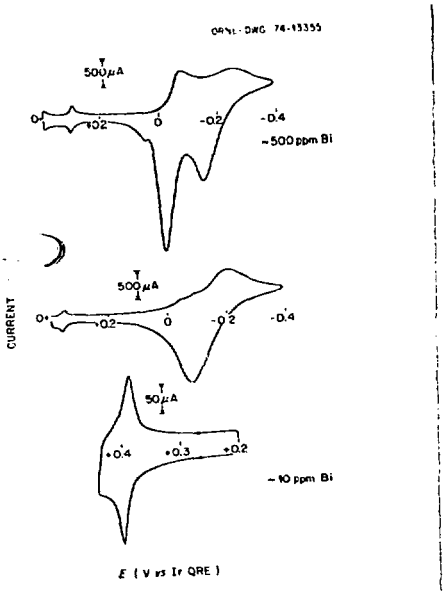

Figure 1. Voltammograms for the reduction of bismuth(III) and nickel(II) at an iridium electrode at 500°C

techniques were used for measurements of lower concentrations of Bi(III) (41). By plating bismuth under controlled conditions of time and potential onto a glassy carbon electrode at a potential sufficiently cathodic to reduce Bi(III) but not Ni(II), and then scanning the potential anodically, the bismuth is stripped from the electrode; the peak height of the anodic stripping curve is a function of the concentration of bismuth. Calibration of the anodic stripping method was achieved by comparing the peak height of the stripping curves to the concentration of bismuth calculated from voltammetry and using linear extrapolation to lower bismuth concentrations. The peak height of the stripping curves is a linear function of plating time (Figure 2). The concentration of bismuth during continued loss from the melt was followed with this technique to sub-ppm (< 25 ppb) concentrations by employing plating times of about 30 min. Longer plating times were not practical due to small signal-to-noise ratios. Also, at longer plating times, the interference of nickel is more severe.

The prewave observed at the iridium electrode (but not at the other working electrodes) did not change appreciably until the bismuth concentration decreased below $\sim$ 1 ppm; then the prewave decreased markedly but not linearly with bismuth concentration. In fact, a small prewave was still observed below the detection limit of bismuth by anodic stripping. This prewave may prove of value as a qualitative indicator of bismuth.

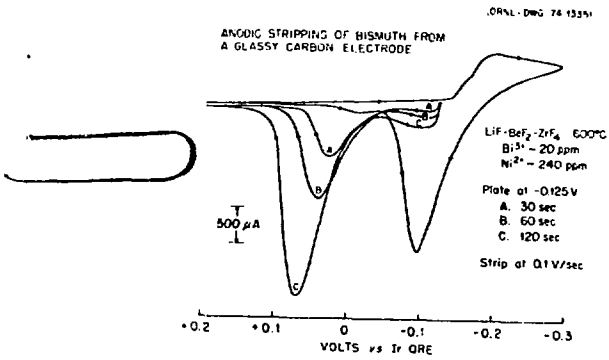

Figure 2. Bismuth stripping curves from a glassy carbon electrode

Iron

Iron(II) is a corrosion product present in molten-salt reactor fuels. We have previously (1,4,23) carried out electrochemical studies of iron(II) in molten LiF-NaF-KF (46.5-11.5-42.0 mole %), LiF-BeF_2-ZrF_4 (69.6-25.4-5.0 mole %), and $NaBF_4$-NaF (92-8 mole %). Since the fuel solvent for the MSBR is a thorium-containing salt, LiF-BeF_2-ThF_4 (72-16-12 mole %), it was of interest to conduct voltammetric and chronopotentiometric studies of iron(II) in this fuel solvent. To determine concentration and/or diffusion coefficients by linear sweep voltammetry, it is necessary to know whether the product of the electrochemical reaction is soluble or insoluble. The measurements discussed below were done with this purpose in mind. A more detailed account of this work has been recently published (31).

A voltammogram showing the reduction of iron(II) at a gold electrode is shown in Figure 3. The circles represent the theoretical shape based on current functions tabulated by Nicholson and Shain (42) for a reversible wave where both the oxidized and reduced forms of the electroactive species are soluble. Thus, even though Fe(II) is reduced to the metal at gold, the electrode reaction very closely approximates the soluble-product case, apparently through the formation of iron-gold surface alloys. Further evidence that the Fe(II) → Fe electrode reaction at gold conforms to the soluble product case is illustrated by the chronopotentiograms in Figure 4. The ratio of the forward to reverse transition times (τ_f/τ_r) compares favorably with the predicted value of 3 (43) for the soluble case, which again points to the formation of surface alloys.

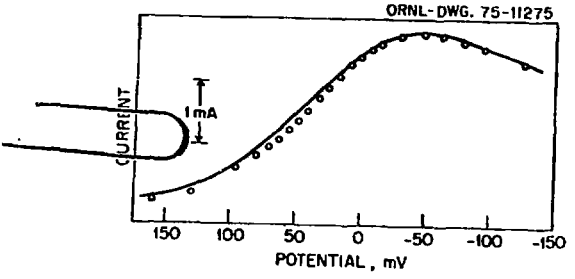

Figure 3. Stationary electrode voltammogram for the reduction of Fe^{2+} at a gold electrode in molten $LiF-BeF_2-ThF_4$. Potential axis is $(E - E_{1/2})/2$. Solid line is experimental. Circles are theoretical shape for soluble product. Iron(II) concentration 0.027 F; electrode area, 0.25 cm^2; temperature, 650°C.

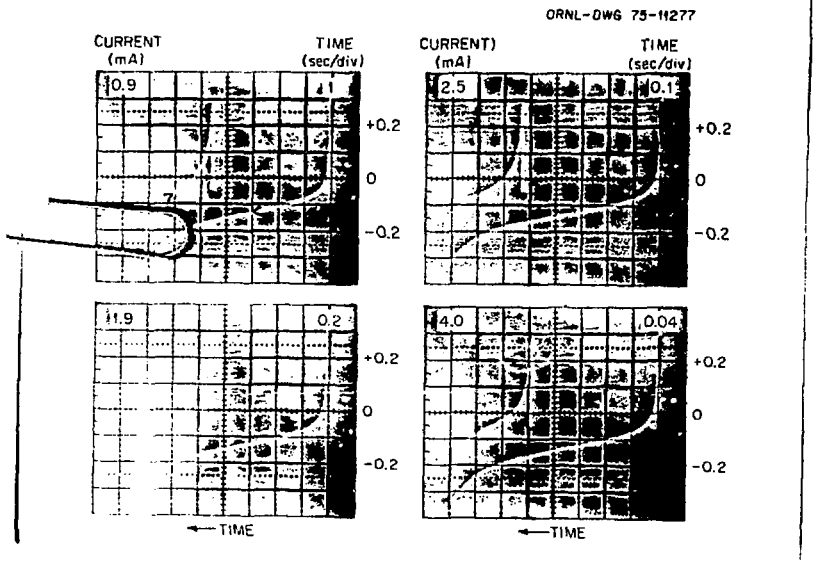

Figure 4. Cyclic chronopotentiograms for the reduction of iron(II) at a gold electrode. Formality of iron(II), 0.15; electrode area, 0.25 cm^2; temperature, 600°C; potential scale, volts vs Ir QRE.

The reduction of Fe(II) at a pyrolytic graphite electrode is illustrated by the chronopotentiograms shown in Figure 5. The ratio of the transition times (τ_f/τ_r) is approximately unity (43), which is indicative that Fe(II) is reduced to metallic iron which

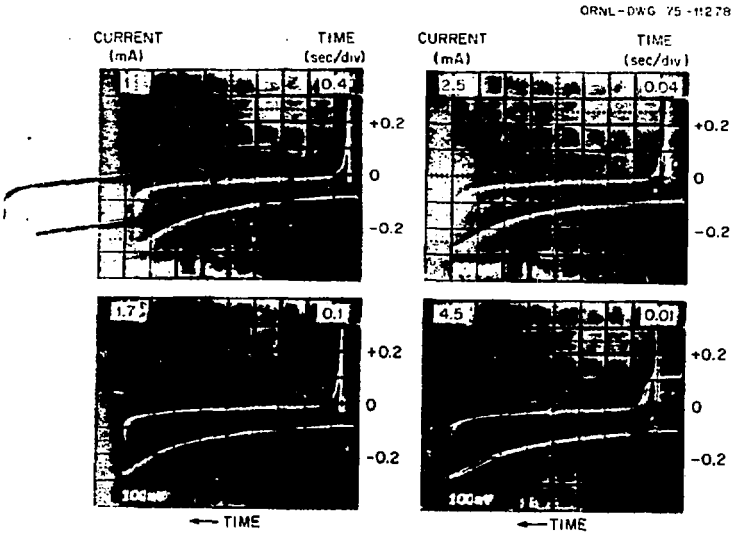

Figure 5. Cyclic chronopotentiograms for the reduction of iron(II) at a pyrolytic graphite electrode. Formality of iron(II), 0.027; electrode area, 0.1 cm^2; temperature, 650°C; potential scale, volts vs Ir QRE.

does not interact with the pyrolytic graphite and that all the iron is stripped from the electrode upon current reversal. The chronopotentiometric results are supported by the voltammetric difference between peak and half-peak potentials, $E_p - E_{p/2}$ (42). The measured $E_p - E_{p/2}$'s are in very good agreement with the predicted values for the reversible deposition of an insoluble substance for n = 2 (5). Therefore, iron appears to be reversibly reduced to a soluble form at gold and to an insoluble material at pyrolytic graphite.

Chronopotentiograms for the reduction of Fe(II) at an iridium electrode at 518 and 600°C are shown in Figure 6. The τ_f/τ_r ratio at 518°C is approximately unity and at 600°C is 3, which is evidence that Fe(II) reduction at iridium approximates the insoluble-species case (as with pyrolytic graphite) at 518°C and the soluble-product case (as with gold) at 600°C. This change in reduction behavior with temperature was not as pronounced at gold or at pyrolytic graphite. Average diffusion coefficients of Fe(II) in this melt evaluated from the chronopotentiometric measurements by means of the Sand equation (44) are approximately 4.2×10^{-6}, 8.0×10^{-6}, and 1.5×10^{-5} cm^2/sec at 518,600, and 700°C, respectively.

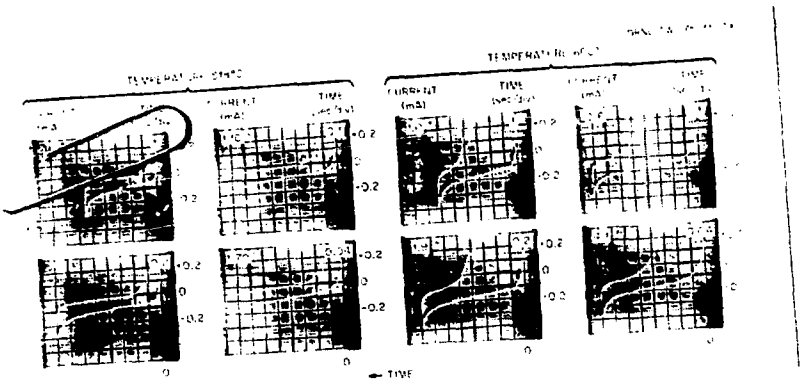

Figure 6. Cyclic chronopotentiograms for the reduction of iron(II) at an iridium electrode. Formality of iron(II), 0.015; electrode area, 0.2 cm^2; potential scale, volts vs Ir QRE.

Tellurium

Tellurium occurs in nuclear reactors as a fission product and results in shallow integranular cracking in structural metals and alloys (45).

Meaningful voltammograms were not obtained following additions of either Li_2Te or $LiTe_3$ (∿50 mg of each in the forms of pressed pellets to ∿800 ml melt) to molten $LiF-BeF_2-ThF_4$ at 650°C. It was later determined that Li_2Te is insoluble in the melt. Chemical analysis indicated < 5 ppm (<0.13mM) Te in the melt while other solubility experiments (46) indicated < 10^{-5} mole fraction (0.3mM) of Te. It was also found that $LiTe_3$ is not stable in the melt under our non-isothermal experimental conditions. This substance apparently decomposes to Li_2Te and Te upon contacting the melt at ∿650°C. According to the spectrophotometric measurements of Bamberger, et al. (47) isothermal conditions were necessary for the continued observation of the absorption band attributed to Te_3^- in $LiF-BeF_2-ZrF_4$; under non-isothermal conditions, the absorption band quickly disappeared with evidence of tellurium metal formation. Behavior of tellurium in molten fluorides has also been studied by Toth (48) using absorption spectrophotometry.

In an effort to obtain additional information on the formation and stability of tellurides under non-isothermal conditions, studies were conducted on the telluride species produced in situ by cathodizing elemental tellurium ($mTe+ne \rightarrow Te_m^{n-}$). Chronopotentiometric and double potential step experiments conducted at a tellurium pool electrode (∿0.1 cm^2) contained in a graphite cup revealed that the telluride species generated does not appear to be stable at ∿ 650°C. Instability was indicated by the chronopotentiometric experiments by comparing the ratio of the forward and

reverse transition times (43). Generation of a stable but insoluble substance yields $\tau_f/\tau_r = 1$; for a soluble and stable species, $\tau_f/\tau_r = 3$ is predicted. For an unstable species, on the other hand, the τ_f/τ_r ratio should be greater than three. For these experiments, the current was reversed at a time $t<\tau_f$; however, the above conclusions remain valid as long as $t\leq\tau_f$; however, the above conclusions remain valid as long as $t\leq\tau_f$. Potential-time curves recorded at the tellurium pool electrode produced $\tau_f/\tau_r>>3$ in all the runs indicating that the telluride species generated is not stable, at least within the time frame of the experiment (seconds).

In the double potential step (49) experiments, the anodic to cathodic current ratio (i_a/i_c) is plotted versus a function of time (f(t)) during which the potential step is applied and removed. For a stable system, $i_a/i_c = 1$ when f(t) is extrapolated to zero (49). For the generation of an unstable species, $i_a/i_c<1$; this was observed for the tellurium experiments. Plots of log i versus E from the potential step experiments revealed an n value close to unity. The validity of n value determinations by this method is discussed by Armstrong, et al. (50) and by Bacarella and Griess (51). Bronstein and Posey (52) also obtained an n value of unity from polarization studies of tellurium in molten chlorides utilizing a different method.

Thus, these results indicate that an unstable telluride species is generated; under non-isothermal conditions, it undergoes a decomposition reaction. Reasonable reaction pathways are as follows:

$$2Te^{-1} \rightarrow Te_2^{2-}$$

$$Te_2^{2-} \rightarrow Te^{2-} + Te\uparrow \quad (m=1)$$

or

$$2Te_m^{-} \rightarrow Te^{2-} + (2m-1)\ Te\uparrow \quad (m>1)$$

The Te^{2-} ion does not appear to be soluble in fluoride melts of these compositions at least to the extent that voltammetric detection is feasible.

Recent spectrophotometric studies (48) indicate that the Te_2^{2-} ion is the most soluble tellurium species in molten fluorides but that it can only be stabilized under isothermal conditions.

Oxide and Related Species

The main purpose of these studies was to develop the basis for an in situ electroanalytical method for the determination of low levels of soluble oxide in MSR fuel streams. The importance of oxide monitoring in a molten salt reactor fuel is that oxide levels must be kept low (< few hundred ppm); otherwise, there is danger of precipitating UO_2 which could form "hot spots" in a reactor system.

We were also interested in establishing the electrooxidation pathway for oxide in these melts, and in this connection we also briefly studied the electrooxidation of peroxide and superoxide ions. It was observed that only at gold electrodes reproducible voltammograms for the oxidation of oxide and related species were observed. A more detailed account of this work appears elsewhere (32); the main conclusions are given below.

Cyclic voltammetric and chronopotentiometric results in molten LiF-BeF_2-ZrF_4 (65.6 - 29.4 - 5.0 mole%) and LiF-BeF_2-ThF_4 (72-16-12 mole%) in the temperature interval 500 - 710°C indicate the following electrochemical reaction pathway:

$$O^{2-} = O + 2e$$

$$O + O = O_2$$

$$O + O^{2-} = O_2^{2-}$$

Some evidence for adsorption of O_2 was obtained. O_2^{2-} ions are oxidized further producing a voltammetric post-wave which increases with Na_2O_2 additions. O_2^{2-} ions gradually decompose in these media; this decomposition is more rapid in Zr(IV)-containing melts as compared to the Th(IV)-containing melts. NaO_2 additions result in the same voltammetric results as obtained upon the addition of Na_2O_2, indicating that O_2^- ions are more unstable in these melts than in the previously studied LiF-NaF-KF eutectic (25).

U(IV)/U(III) Ratio Determinations

The corrosion of Hastelloy N and other structural materials by MSF type fuels containing UF_4, has been attributed (53) to temperature gradient mass transfer of the most active constituent of the alloy which is chromium. The reaction is represented as

$$2UF_4 + Cr \rightarrow CrF_2 + 2UF_3.$$

The extent of this reaction is controlled by the activity of chromium in the alloy, the UF_4/UF_3 ratio in the salt and the concentration of dissolved CrF_2.

These studies were carried out in collaboration with Metals and Ceramics Division and Reactor Division personnel at the Oak Ridge National Laboratory and represent the first use of controlled potential voltammetry for molten salt corrosion studies. The principle of the voltammetric U(IV)/U(III) ratio determination (15) is illustrated in Figure 7. For these measurements, the counter electrode is the molten salt loop (see below); two iridium electrodes comprise the quasi-reference and working electrodes, respectively. Voltammograms of the U(IV) → U(III) electrode reaction are recorded relative to the Ir ORE which is poised at the equilibrium potential (E_{eq}) of the melt. This potential, in turn, is governed by the U(IV)/U(III) ratio. From the difference between E_{eq} and $E_{1/2}$ which is the voltammetric equivalent of E°, the U(IV)/U(III) ratio can be calculated from the Nernstian relationship.

In-line monitoring of the U(IV)/U(III) ratio in several corrosion test loops was carried out over a period of about two years. A schematic drawing of a loop system is shown in Figure 8. The loop portion of the assembly is constructed of Hastelloy N tubing and is heated on the bottom and left vertical side. By cooling the other two sides, the molten salt can be made to flow by density differences; thus, the term thermal convection loop. The corrosion test loops ranged from thermal convection loops of modest size to large pump driven forced convection loops. They were designed to approximate flow characteristics and temperature gradients of an MSBR. Other important features of the loops were removable corrosion specimens and ports for insertion of electrodes for voltammetric measurements.

The use of voltammetry to provide in-line measurements of the oxidation potential and corrosion product indicators in the salt is illustrated by Figure 9, in which both the current-voltage curve and its derivative are presented. In general, well defined and reproducible voltammograms were obtained. The Cr(II) → Cr reduction wave occurs at the foot of the U(IV) reduction wave which makes precise chromium measurements difficult. Efforts to increase the sensitivity of the chromium measurements by plating and stripping techniques produced unexpected phenomena. As noted in the upper curves of Figure 9, the peak height of the stripping curve for a given plating time is critically dependent on the plating potential. It appears that plating chromium in the presence of U(IV) at potentials much more negative than the peak potential for the Cr(II) → Cr reduction wave, the concentration of U(III) at the electrode surface is sufficient to reduce part of the Cr(II)

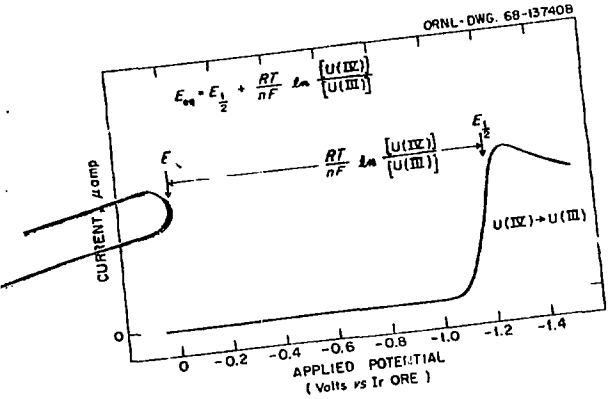

Figure 7. Determination of U(IV)/U(III) ratio by voltammetry

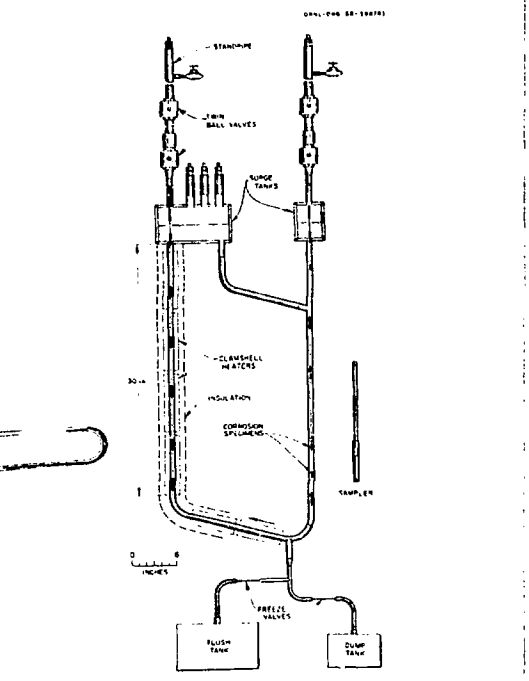

Figure 8. Thermal convection loop schematic*

---

*This Figure was originally presented at the 149th Spring Meeting of The Electrochemical Society, Inc. and is included in the publication PROCEEDINGS OF THE INTERNATIONAL SYMPOSIUM ON MOLTEN SALTS of The Electrochemical Society, Inc.

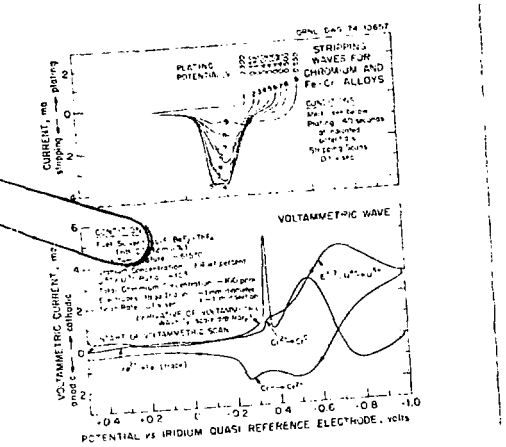

Figure 9. Typical direct and stripping voltammograms for uranium and chromium in MSBR Fuel Salt.

diffusing in before it is reduced by the electrode. Thus the choice of plating potentials for chromium plating and stripping experiments is relatively crucial. Nevertheless, by following relative changes in the chromium linear scan and derivative waves, useful information can be realized on the behavior of Cr(II) in these melts. Either the linear scan or derivative voltammograms can be used for $E_{1/2}$ determinations from which the U(IV)/U(III) ratio is calculated.

The variation of the U(IV)/U(III) ratio with time for two different loop materials, Hastelloy N and Inconel, is illustrated in Figures 10 and 11, respectively. For the Hastelloy N, the U(IV)/U(III) ratio reaches equilibrium at ∿100 whereas for Inconel (an alloy with a higher chromium content) the melt becomes much more reducing (U(IV)/U(III) < 10). Small perturbations usually occurred when specimens were inserted, due to an inadvertent addition of traces of moisture at the same time. These fluctuations, however, were considered to be small enough that they did not affect corrosion measurements (30).

It should be noted that in addition to the advantages of less time and expense, the in-line monitoring techniques provide information not attainable by discrete sampling methods. The in-line monitoring of the U(IV)/U(III) ratio serves as a notable example. This ratio is prohibitively sensitive to atmospheric contamination during sampling and any subsequent sample transfers to hot cells, and is rather meaningless on frozen samples because the ratio undergoes changes during cooling as a result of equilibrium shifts. We also demonstrated the feasibility of completely automating this procedure for the U(IV)/U(III) determination with a dedicated PDP-8

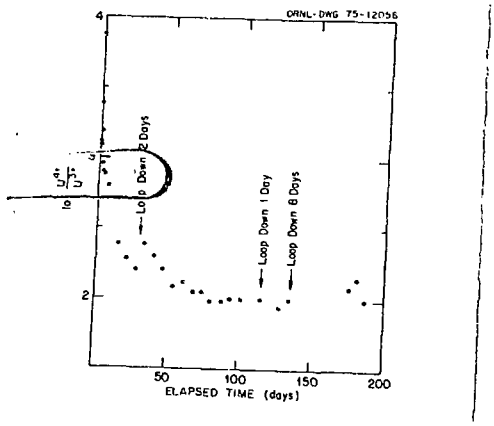

Figure 10. Log (IV)/U(III) vs elapsed time for forced convection Hastelloy N Loop.

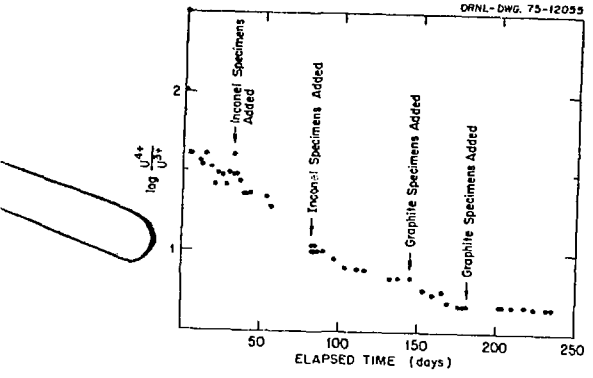

Figure 11. Log U(IV)/U(III) vs elapsed time for thermal convection Inconel Loop.

computer (54) which operates the voltammeter, analyzes the data, and computes the U(IV)/U(III) ratio.

4. SUMMARY

Electroanalytical studies were carried out on BiF_3 in molten $LiF-BeF_2-ZrF_4$. Trace levels of bismuth are expected to occur in an MSR fuel stream from reprocessing operations. Voltammetric measurements were also made in the presence of NiF_2, an anticipated interference. Limits of detection were about 10 ppm by linear scan voltammetry but could be extended to much lower levels (< 25 ppb)

by anodic stripping techniques. Stable melts containing Bi(III) cannot be maintained because bismuth is slowly lost from the melt by volatilization as BiF_3.

To determine concentration and/or diffusion coefficients by linear sweep voltammetry, it is necessary to know whether the product of the electrochemical reaction is soluble or insoluble. It was observed from voltammetry and chronopotentiometry that the $Fe(II)+2e \rightarrow Fe$ electrode reaction in molten $LiF-BeF_2-ThF_4$ closely approximates the soluble product case at a gold electrode, the insoluble product case at pyrolytic graphite, and, depending on the temperature, both soluble and insoluble product cases at an iridium electrode.

Voltammetric measurements were made in molten $LiF-BeF_2-ThF_4$ following additions of Li_2Te and $LiTe_3$ in an effort to identify soluble electroactive tellurium species. No voltammetric evidence for such compounds was obtained. Electrochemical studies were carried out on the tellurium species generated in situ in molten $LiF-BeF_2-ThF_4$ when a tellurium electrode is cathodized; the results indicated that the species generated is of the type Te_m^- ($m>1$) and appears to be unstable under the existing experimental conditions.

We have shown that the electrooxidation of soluble oxide species at gold electrodes in fluoride melts, such as $LiF-BeF_2-ZrF_4$ and $LiF-BeF_2-ThF_4$, provides the basis for an in situ determination of small amounts of dissolved oxide. The electrooxidation results in atomic oxygen which rapidly combines to form chemisorbed O_2 or reacts with the reactant O^{2-} forming O_2^{2-} which is oxidized further.

In-line monitoring of U(IV)/U(III) ratios was carried out for both thermal-convection and forced-convection corrosion test loops. The U(IV)/U(III) ratio reflects the redox condition of the fuel salt and stabilizes at ~100 in loops constructed of Hastelloy N. The melt is more reducing, however, in an Inconel loop. In addition to the saving of time and expense by in-line electroanalytical techniques, information which cannot be achieved by discrete sampling methods can be obtained.

5. ACKNOWLEDGMENTS

We gratefully acknowledge assistance from and valuable discussions with the following: J. R. Keiser of the Metals and Ceramics Division and W. R. Huntley, Reactor Division, Oak Ridge National Laboratory who were in charge of the thermal convection loops and forced convection corrosion test loops, respectively; T. R. Mueller of the Instrumentation Group, Analytical Chemistry Division, who played a very important role in the area of instrumentation design and modifications, as well as A. S. Meyer, Jr. and

J. M. Dale of the Analytical Chemistry Division who were mainly responsible for automating the U(IV)/U(III) ratio determination procedure.

6. POSTSCRIPT

We note with great sadness that A. S. Meyer, Jr., Group Leader in charge of Analytical Research and Development associated with the Molten Salt Breeder Reactor Program, passed away in December 1975.

The Molten Salt Breeder Reactor Program at the Oak Ridge National Laboratory was terminated in June 1976.

7. REFERENCES

(1) D. L. Manning, J. Electroanal. Chem., 6, 227 (1963).

(2) D. L. Manning and G. Mamantov, J. Electroanal. Chem., 6, 328 (1963).

(3) D. L. Manning, J. Electroanal. Chem., 7, 302 (1964).

(4) D. L. Manning and G. Mamantov, J. Electroanal. Chem., 7, 102 (1964).

(5) G. Mamantov, D. L. Manning, and J. M. Dale, J. Electroanal. Chem., 9, 253 (1965).

(6) D. L. Manning, J. M. Dale, and G. Mamantov, in Polarography, 1964, G. J. Hills, ed., Vol. 2, p. 1143, MacMillan, London, 1966.

(7) G. Mamantov and D. L. Manning, Anal. Chem., 38, 1494 (1966).

(8) J. P. Young, G. Mamantov, and F. L. Whiting, J. Phys. Chem., 71, 782 (1967).

(9) D. L. Manning and G. Mamantov, J. Electroanal. Chem., 17, 137 (1968).

(10) G. Mamantov and D. L. Manning, J. Electroanal Chem., 18, 309 (1968).

(11) H. W. Jenkins, G. Mamantov, and D. L. Manning, J. Electroanal. Chem., 19, 385 (1968).

(12) H. W. Jenkins, Jr., "Electrochemical Measurements in Molten Fluorides," Ph.D. Dissertation, The University of Tennessee, March 1969.

(13) G. Mamantov, in Molten Salts; Characterization and Analysis, G. Mamantov, ed., M. Dekker, New York, N.Y. 1969.

(14) D. L. Manning and J. M. Dale, in Molten Salts: Characterization and Analysis, G. Mamantov, ed., M. Dekker, New York, N.Y. 1969.

(15) H. W. Jenkins, G. Mamantov, D. L. Manning, and J. P. Young, J. Electrochem. Soc., 116, 1712 (1969).

(16) H. W. Jenkins, G. Mamantov, and D. L. Manning, J. Electrochem. Soc., 117, 183 (1970).

(17) F. L. Whiting, "Studies of the Superoxide Ion and Other Solute Species in Molten Fluorides," Ph.D. Dissertation, The University of Tennessee, August 1970.

(18) D. L. Manning and G. Mamantov, High Temp. Sci., 3, 533 (1971).

(19) F. R. Clayton, Jr., "Electrochemical Studies in Molten Fluorides and Fluoroborates," Ph.D. Dissertation, The University of Tennessee, March 1972.

(20) H. R. Bronstein and D. L. Manning, J. Electrochem. Soc., 119, 125 (1972).

(21) F. R. Clayton, Jr., G. Mamantov, and D. L. Manning, J. Electrochem. Soc., 120, 1193 (1973).

(22) F. R. Clayton, Jr., G. Mamantov, and D. L. Manning, J. Electrochem. Soc., 120, 1199 (1973).

(23) F. R. Clayton, Jr., G. Mamantov, and D. L. Manning, High Temp. Sci., 5, 358 (1973).

(24) G. Ting, "Thermodynamic and Electrochemical Studies of Niobium in Molten Fluorides and Chloroaluminates," Ph.D. Dissertation, The University of Tennessee, August 1973.

(25) F. L. Whiting, G. Mamantov, and J. P. Young, J. Inorg. Nucl. Chem., 35, 1553 (1973).

(26) J. S. Hammond and D. L. Manning, High Temp. Sci., 5, 50 (1973).

(27) D. L. Manning and G. Mamantov, Electrochim. Acta, 19, 177 (1974).

(28) F. R. Clayton, Jr., G. Mamantov, and D. L. Manning, J. Electrochem. Soc., 121, 86 (1974).

(29) G. Mamantov, B. Gilbert, K. W. Fung, R. Marassi, P. Rolland, G. Torsi, K. A. Bowman, D. L. Brotherton, L. E. McCurry, and G. Ting, in Proceedings of the International Symposium on Molten Salts, J. P. Pemsler, ed., The Electrochemical Society, Princeton, New Jersey, 1976, pp. 234-239.

(30) J. R. Keiser, D. L. Manning, and R. E. Clausing, in Proceedings of the International Symposium on Molten Salts, J. P. Pemsler, ed., The Electrochemical Society, Inc., Princeton, New Jersey, 1976, pp. 315-323.

(31) D. L. Manning and G. Mamantov, High Temp. Sci., 8, 219 (1976).

(32) D. L. Manning and G. Mamantov, J. Electrochem. Soc., 124, 480 (1977).

(33) M. W. Rosenthal, P. N. Haubenreich, and R. B. Briggs, Oak Ridge National Laboratory Report, ORNL-4812 (1972).

(34) T. R. Mueller and H. C. Jones, Chem. Instrum., 2, 65 (1969).

(35) J. H. Shaffer, et al., Oak Ridge National Laboratory Report, ORNL-3951 (1964).

(36) B. Gilbert, G. Mamantov, and G. M. Begun, Inorg. Nucl. Chem. Letters, 10, 1123 (1974).

(37) C. E. Bamberger, H. F. McDuffie and C. F. Baes, Jr., Nucl. Sci. and Eng., 22, 14 (1965).

(38) D. Y. Valentine and A. D. Kelmers, Oak Ridge National Laboratory Report, ORNL-5078, 29 (1975).

(39) L. E. McNeese in ref. 33, p. 331.

(40) D. Cubicciotti, J. Electrochem. Soc., 115, 1138 (1968).

(41) A. S. Meyer, et al., Oak Ridge National Laboratory Report, ORNL-5047, 56 (1975).

(42) R. S. Nicholson and I. Shain, Anal. Chem., 36, 706 (1964).

(43) W. H. Reinmuth, Anal. Chem., 32, 1514 (1960).

(44) P. Delahay, New Instrumental Methods in Electrochemistry, Interscience, New York, 1954, p. 184.

(45) H. E. McCoy, in ref. 33, p. 207.

(46) D. Y. Valentine and A. D. Kelmers, Oak Ridge National Laboratory Report, ORNL-5132, 24 (1976).

(47) C. E. Bamberger, J. P. Young, and R. G. Ross, J. Inorg. Nucl. Chem., 36, 1158 (1974).

(48) L. M. Toth, Abstract ANAL-54, American Chemical Society Meeting, San Francisco, Calif., August 29-September 3, 1976.

(49) R. W. Murray, in Physical Methods of Chemistry, Part IIA: Electrochemical Methods, A. Weissberger and B. W. Rossiter, eds., Wiley-Interscience, 1971, p. 601.

(50) R. D. Armstrong, T. Dickinson, and K. Taylor, J. Electroanal. Chem., 64, 155 (1975).

(51) A. L. Bacarella and J. C. Griess, Jr., J. Electrochem. Soc., 120, 459 (1973).

(52) H. R. Bronstein and F. A. Posey, Oak Ridge National Laboratory Report, ORNL-5132, 29 (1976).

(53) W. R. Grimes, in reference 33, p. 111.

(54) A. S. Meyer, et al., Oak Ridge National Laboratory Report, ORNL-4449, 157 (1969).